Available online at www.sciencedirect.com
ScienceDirect
Trans. Nonferrous Met. Soc. China 34(2024) 3650−3661
Transactions of Nonferrous Metals Society of China
www.tnmsc.cn

Growth kinetics of interfacial intermetallic compounds formed in SnPbInBiSb high entropy alloy soldered joints on Cu substrates

Shuai WANG[1], Jia-yun FENG[1], Wei WANG[1], Wen-chao CAO[2], Xin DING[2], Shang WANG[1], Yan-hong TIAN[1,3]

1. State Key Laboratory of Precision Welding and Joining of Materials and Structures, Harbin Institute of Technology, Harbin 150001, China;
2. National Key Laboratory for Precision Hot Processing of Metals, Harbin Institute of Technology, Harbin 150001, China;
3. Zhengzhou Research Institute, Harbin Institute of Technology, Zhengzhou 450041, China

Received 1 March 2023; accepted 28 September 2023

Abstract: The growth behavior of the complex intermetallic compounds (IMCs) formed at the interface of Cu/SnPbInBiSb high entropy alloy solder joints was explored. The growth inhibition mechanism of the IMCs at the Cu/SnPbInBiSb solid−liquid reaction interface was revealed. The results showed that the growth rate of the complex IMCs obviously decreased at the Cu/SnPbInBiSb solid−liquid reaction interface. The maximum average thickness of IMCs only reached up to 1.66 μm after reflowing at 200 °C for 10 min. The mechanism for the slow growth of the complex IMCs was analyzed into three aspects. Firstly, the high entropy of the liquid SnPbInBiSb alloy reduced the growth rate of the complex IMCs. Secondly, the distorted lattice of complex IMCs restrained the diffusion of Cu atoms. Lastly, the higher activation energy (40.9 kJ/mol) of Cu/SnPbInBiSb solid−liquid interfacial reaction essentially impeded the growth of the complex IMCs.

Key words: high entropy alloy; interfacial reaction; microstructure evolution; growth kinetics; intermetallic compounds

1 Introduction

With the fast development of advanced chip technology and electronic packaging technology, three-dimensional integrated circuit (3D IC) is thriving and prosperous in the microelectronic industry [1,2]. In 3D IC, the dies are vertically connected by through-silicon-via (TSV), micro-bump, controlled-collapse-chip-connection (C4) and ball-grid-array (BGA). It is a common sense that the lifetime of 3D IC is highly dependent on the reliability of these solder joints [3]. Considering the convenience in the interconnection of different components in 3D IC, these solder joints are connected in a hierarchy of melting temperature [4]. Thus, the former solder joints would not be melted during the reflowing process of the next level solder joints. In this hierarchy, the solder alloy can be divided into three levels [4,5]. The first level of solder has the highest melting temperature over 300 °C, such as the high-Pb solder 95Pb5Sn. The melting temperature of the second level solder is around 200 °C, which includes eutectic SnPb and eutectic Sn−Ag or Sn−Ag−Cu solder. Then, the third level of solder has a lower melting temperature below 150 °C, such as the eutectic Sn−Bi solder. Moreover, the widespread application of high-melting-temperature solder usually results in the warpage of Si interposer and affects the thermal stability of polymer substrate [5]. With the increase of chip size, the warpage issue has become

Corresponding author: Jia-yun FENG, E-mail: fengjy@hit.edu.cn;
Yan-hong TIAN, Tel: +86-451-86418359, E-mail: tianyh@hit.edu.cn
DOI: 10.1016/S1003-6326(24)66631-8

more and more serious during the multiple reflow process, thus weakening the reliability of the integrated circuit [3,6]. To relieve this warpage issue, the low-melting-temperature solders such as eutectic Sn−Bi were applied. The application of eutectic Sn−Bi solder can reduce the thermal stress caused by the mismatched thermal expansion coefficients between the solder joints and the substrates [7,8].

However, the eutectic Sn−Bi solder joint has a poor ductility and frangibility [9]. The Bi element tends to increase the brittleness of the Sn-based solder [10] and segregate at the reaction interface between the Cu substrate and solder, which further deteriorates the mechanical properties of the solder joints [11]. To optimize the comprehensive properties of Sn−Bi solder, many researches were carried out. ZHU et al [12] added the Al_2O_3 nanoparticles into the Sn58Bi solder and found that the grains of Sn58Bi solder were refined. Apart from Al_2O_3, Ni, Cu_6Sn_5, Mo and Cu nanoparticles could also enhance the heterogeneous nucleation and refine the microstructure of the Sn−Bi solder [13−16]. XU et al [17] and SONG et al [18] found that the doping of Ag, Ni, Co, Cu and Cr elements could increase the mechanical properties of Sn−Bi solders. MA et al [19] doped the graphene nanosheets into the Sn−Bi solder and found that the tensile properties of Sn−Bi solder were enhanced. Furthermore, the growth behavior of intermetallic compound (IMC) formed in Sn−Bi solder joints was investigated. LI et al [20] found that the doping of Cu, Si, Al, Nb, Pt, Cr, Zn, Ag and Au elements into Sn−Bi solder could suppress the growth of IMC. Researchers also found that nanoparticles such as Ti, ZrO_2 and CuZnAl particles tended to segregate at the IMC grain surface or phase boundary and could inhibit the diffusion behavior of reaction atoms, thus restraining the overgrowth of IMC. But the effect of these doping ways to enhance the comprehensive properties of binary Sn−Bi solder was restricted. The doped elements or particles cannot completely solve the frangibility and segregation of Bi phase.

Considering the excellent properties of high entropy alloy [21,22], researchers introduced the concept of high entropy alloy into solder alloy and investigated the solderability of these high entropy solder alloys. LIU et al [5] fabricated the medium entropy alloy SnBiInZn, and then studied the microstructure and wetting behavior of SnBiInZn solder, as well as the growth kinetics of IMC and shear properties of Cu/SnBiInZn/Cu solder joints. They found that the medium entropy alloy SnBiInZn has good wetting ability and low melting temperature of 80 °C. Furthermore, the interfacial reaction between SnBiInZn and Cu was very slow and the formed IMC layer was very thin, which was caused by the fact that the high configurational entropy of SnBiInZn solder alloy could lead to the very low reaction kinetics. Our previous work [23,24] also proved the slow interfacial reaction between high entropy solder alloy SnPbInBiSb and Cu substrate, but the reason for the low growth rate of IMC needs more exploration. In this work, the interfacial microstructure evolution and the growth kinetics of the complex IMC formed in Cu/SnPbInBiSb/Cu sandwich solder joints were investigated. The component of the complex IMC and the diffusion behavior of Cu/SnPbInBiSb solid−liquid reaction interface were also explored. More importantly, the mechanism of the slow growth of the complex IMC layer was revealed.

2 Experimental

The high entropy solder alloy SnPbInBiSb was prepared with pure metals Sn, Pb, In, Bi and Sb (purity >99.995%). As shown in Fig. 1, Sn, In and Bi elements were ordinary candidates for lead-free solder, while the Pb element was still required in solder joints for the high-reliability application in the industry of aerospace field. The addition of Pb and Sb elements could also increase the fatigue resistance and ductility of the solder joints. Thus, Sn, Pb, In, Bi and Sb elements were chosen as the components of the high entropy alloy. These metals were mixed at an equal-atomic ratio and melted in the graphite crucible of a resistance furnace with an argon atmosphere. The melting temperature was set at 680 °C, and the heating rate was 10 °C/min. To improve the uniformity of the chemical composition, the melting process was repeated five times and stirred with stainless-steel bar at intervals of 5 min. Then, the prepared solder alloy was cut into pieces with the thickness of about 0.1 mm. The copper substrates with dimensions of 3 mm × 3 mm × 1 mm were ground and polished. The Cu/SnPbInBiSb/Cu sandwich solder joints were assembled and reflowed with a heating plate

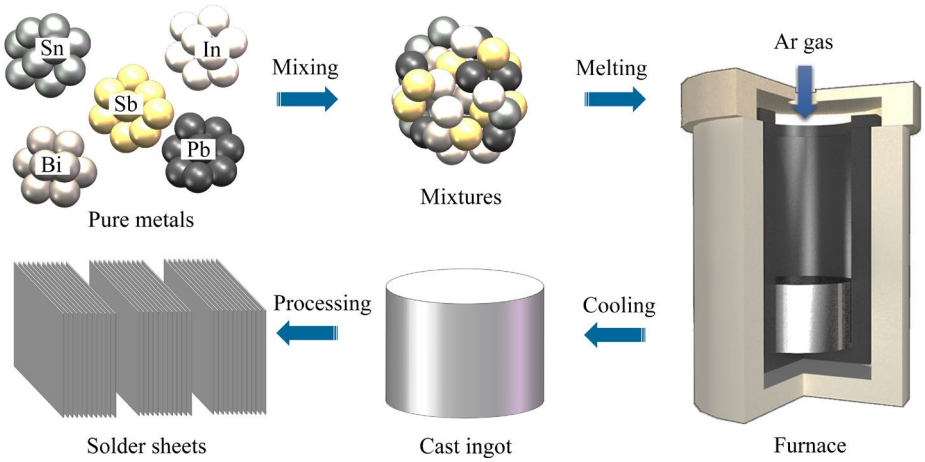

Fig. 1 Fabrication process of SnPbInBiSb solder alloy

(JF966-100, China) at 160, 180, and 200 °C for 1, 5, and 10 min, respectively. To keep the width of solder seams in different solder joints consistent with each other, these solder joints were reflowed under the same load of 50 g.

The reflowed solder joints were mounted and polished for the microstructure characterization. The phase components of SnPbInBiSb were detected by X-ray diffraction (XRD, Bruker AXS D8 ADVANCE, Germany). Then, the microstructure of SnPbInBiSb was investigated by the scanning electron microscopy (FIB-SEM, TESCAN AMBER, Czech) and the chemical compositions of the intermetallic compounds were detected by the energy dispersive X-ray (EDX). To reveal the growth kinetics of the IMC, the average thickness of IMC was measured in the pictures of low magnification by ImageJ software. The thin foil sample for the transmission electron microscope experiment was also prepared by focused ion beam equipment (FIB-SEM, TESCAN AMBER, Czech). The brightfield phase, darkfield phase and selected area electron diffraction (SAED) of the prepared thin foil were observed by the scanning transmission electron microscope (STEM, Talos F200X G2, American). The SAED patterns of different phases were indexed by a free software CrysTBox which can automatically index the SAED pattern with high accuracy.

3 Results and discussion

3.1 Microstructures of high entropy solder alloy SnPbInBiSb

The basic properties of SnPbInBiSb solder alloy were investigated in our previous work [23,24], in which the melting temperature and wetting angle of SnPbInBiSb were 112.8 °C and 39.8°, respectively. These basic properties of SnPbInBiSb indicate that this solder alloy has potential to serve as a low-temperature solder alloy. The microstructure and phase components of SnPbInBiSb were detected, as shown in Fig. 2. SnPbInBiSb alloy was composed of SnPbBi phase, Sn-rich solid solution (SS) and InSb phase. The results of our previous

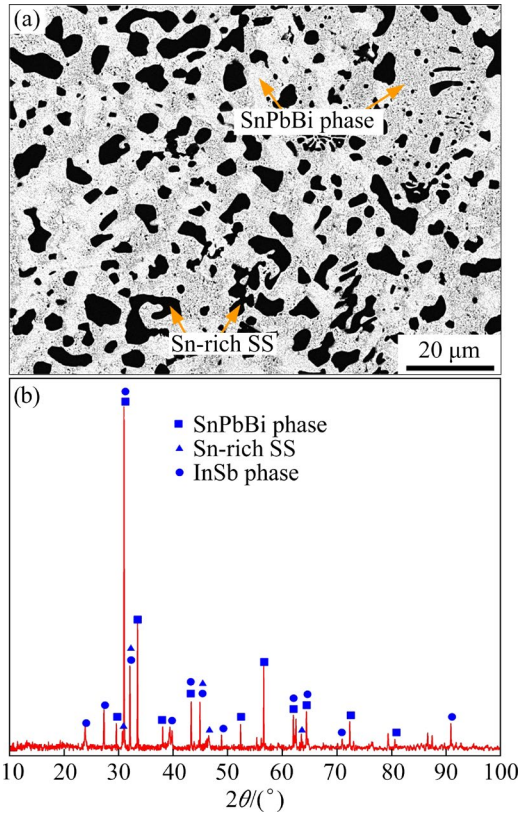

Fig. 2 Microstructure (a) and XRD pattern (b) of SnPbInBiSb solder alloy

work [23,24] showed that the SnPbBi phases could be actually divided into the Pb-rich (grey phase) and Bi-rich (white phase) phases, and the existence of InSb phase had a negligible influence on the interfacial reaction between SnPbInBiSb and Cu. Due to the segregation of In and Sb, the chemical composition of the detected area might be biased but the properties of SnPbInBiSb alloy almost were unchanged. In Fig. 3, SnPbInBiSb solder alloy pieces were assembled with Cu substrates to form sandwich solder joints. These Cu/SnPbInBiSb/Cu sandwich solder joints were reflowed under the same pressure as shown in Fig. 3(a). After reflow, the intersecting surfaces of these solder joints were observed and the average width of the solder seam was 67 μm as shown in Fig. 3(b).

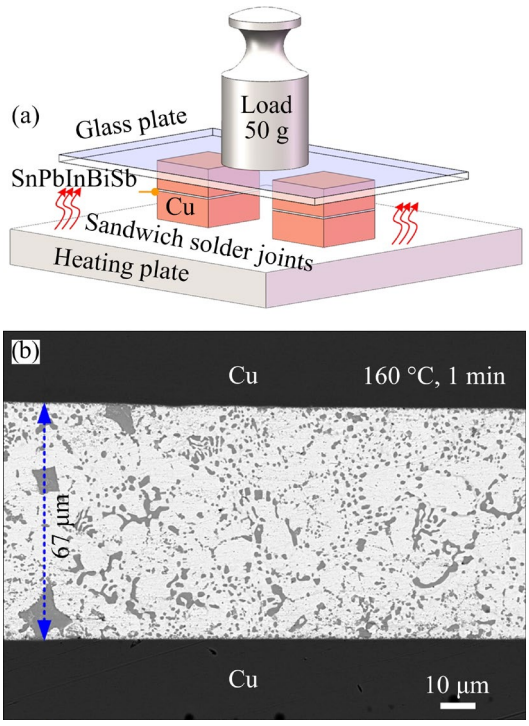

Fig. 3 Fabrication of Cu/SnPbInBiSb/Cu sandwich solder joints: (a) Schematic diagram of reflow process; (b) Microstructure of reflowed solder joint

3.2 Growth behavior of intermetallic compounds

As shown in Fig. 4, the interfacial microstructure of Cu/SnPbInBiSb/Cu sandwich solder joints and the chemical composition of IMC were displayed correspondingly. Figures 4(a−c) display the microstructure evolution along the interface of the solder joints reflowed at 160 °C. It is clear that the slim columnar IMC was formed along the reaction interfaces. Then, these columnar IMCs were gradually coarsened with the increase of reflowing time, rather than forming the lamellar microstructure. The chemical composition of IMC formed along the Cu/SnPbInBiSb interface was detected by EDX and the results of the representative points were listed in Table 1. The results showed that the IMCs in the solder joints reflowed at 160 °C for different durations were both composed of Cu, Sn, Pb, In, Bi and Sb. The major elements of IMC were still Cu and Sn. The average thickness of IMC was measured and the maximum thickness of IMC reached up to 1.04 μm after reflowing at 160 °C for 10 min. Figures 4(d−f) show the microstructure evolution of the solder joints reflowed at 180 °C. It is clear that the microstructure evolution of IMC formed at 180 °C was similar with that formed at 160 °C. The slim columnar IMC grains were gradually coarsened and intersected with the adjacent IMC. Moreover, due to the higher reflowing temperature, the growth of IMC was promoted and the maximum thickness of IMC reached up to 1.49 μm. As shown in the blue circle of Fig. 4(f), the white phase is possibly Bi phase which tended to diffuse into the interface between IMC and Cu substrate [25]. The interfacial microstructure of sandwich solder joints reflowed at 200 °C was shown in Figs. 4(g−i). With the increase of reflowing temperature, the initial microstructure of IMC grains changed into scalloped type. However, when the reflowing time increased, the coarsened columnar structure of IMC still showed up. Under the effect of high reflowing temperature, more reaction atoms acquired enough energy to diffuse. Thus, the growth of IMC was further accelerated and the maximum average thickness of IMC reached up to 1.66 μm. Furthermore, the diffusion of Bi-rich phase was enhanced and a certain amount of Bi-rich phase showed up in the solder joints reflowed at 200 °C only for 5 min. The ratios of elements in the IMC formed in solder joints reflowed at 200 °C was still close to the composition of Cu_6Sn_5. Generally, with the increase of reflowing temperature and reflowing time, the thickness of IMC gradually increased and the type of IMC was seemingly unchanged due to the insufficient proof of the formation of Cu_3Sn, but the diffusion of Bi-rich phase was also enhanced.

The researches about the reaction rates of Cu/Sn-based solder interface were also conducted and summarized in order to evaluate the growth rate

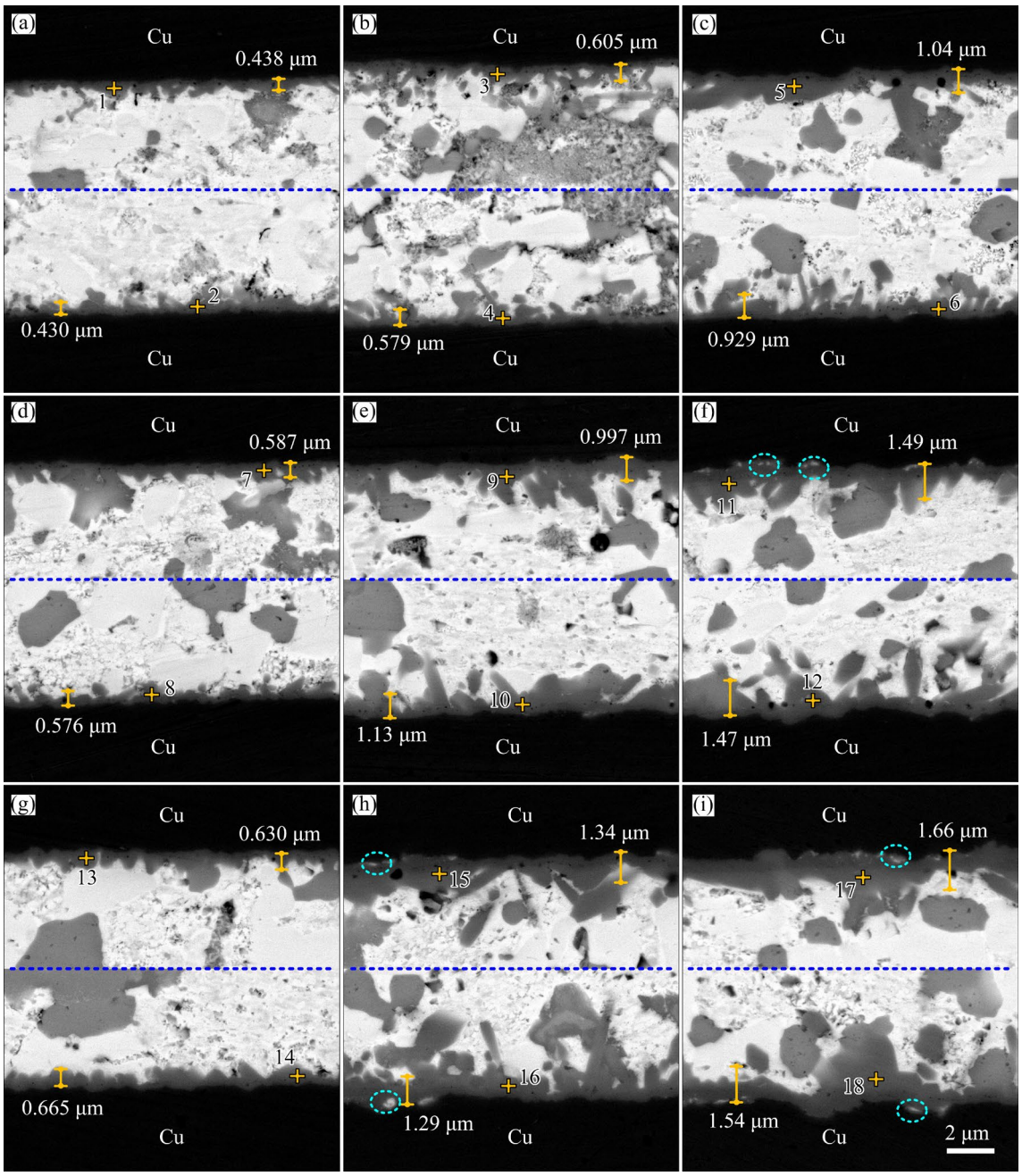

Fig. 4 Interfacial microstructures of solder joints reflowed at different parameters: (a) 160 °C, 1 min; (b) 160 °C, 5 min; (c) 160 °C, 10 min; (d) 180 °C, 1 min; (e) 180 °C, 5 min; (f) 180 °C, 10 min; (g) 200 °C, 1 min; (h) 200 °C, 5 min; (i) 200 °C, 10 min

of IMC formed at Cu/SnPbInBiSb interface. According to the literature reviews, the average thickness of IMC layer at the Cu/SAC305 interface after reflowing at 245 °C for 45 s is 2.7 μm [26], and the average thickness of IMC layer at Cu/Sn interface after reflowing at 250 °C for 1 min is 2.8 μm [27]. The average thickness of IMC at the Cu/Sn−58Bi interface after reflowing at 200 °C (62 °C higher than the melting point of Sn−58Bi) for 1 min is 0.69 μm [28]. As for the Cu/Sn−90Pb and Cu/Sn−5Sb interfaces, the average thickness of IMC layer was respectively about 1 and 1.5 μm after reflowing at 310 and 270 °C for 1 min [29]. Nevertheless, the average thickness of IMC layer formed at Cu/SnPbInBiSb interface after reflowing at 200 °C for 1 min was only 0.648 μm. Compared with the average thickness of IMC layer in common Sn-based solder joints, the growth rate of IMC in Cu/SnPbInBiSb/Cu sandwich solder joints was relatively slow. It is apparent that the SnPbInBiSb

Table 1 Chemical compositions of representative points in Fig. 4 (at.%)

Point No.	Cu	Sn	Pb	In	Bi	Sb
2	48.20	39.14	6.99	0.28	3.93	1.45
3	51.90	36.95	5.15	0.78	3.80	1.41
5	56.19	38.30	1.78	0.54	1.03	2.16
7	54.66	33.91	1.03	2.40	3.23	4.77
10	57.22	34.73	2.66	0.32	2.14	2.92
12	57.73	36.10	1.05	0.91	0.69	3.53
14	56.27	30.99	5.45	0.69	2.59	4.01
15	58.76	35.34	1.13	0.65	0.71	3.41
17	53.43	39.57	2.11	0.52	1.50	2.87

solder alloy could certainly hinder the growth behavior of IMC and reduce the thickness of IMC layer. But the reason why SnPbInBiSb solder could effectively control the growth of IMC needs further exploration. Generally, the growth rate of IMC is highly related to the content of Sn in the solder joints because Cu−Sn reaction dominated the soldering process. Under the same reflowing parameters, the lower content of Sn means lower reaction rate. Theoretically, the content of Sn in the SnPbInBiSb is 20 at.% (15.6 wt.%). However, this relatively high content of Sn in the SnPbInBiSb did not result in the fast growth of IMC. On the contrary, the growth rate of IMC in the SnPbInBiSb solder joints is much lower than that in Sn−90Pb solder joints [29]. Therefore, the slow growth of IMC was not only related to the low content of Sn, but also concerned with other factors.

To further reveal the mechanism of the slow growth of IMC, the elemental distribution of different solder joints was investigated, as shown in Fig. 5. It is clear that the IMC layers in all the solder joints were both rich in Cu, Sn and Sb

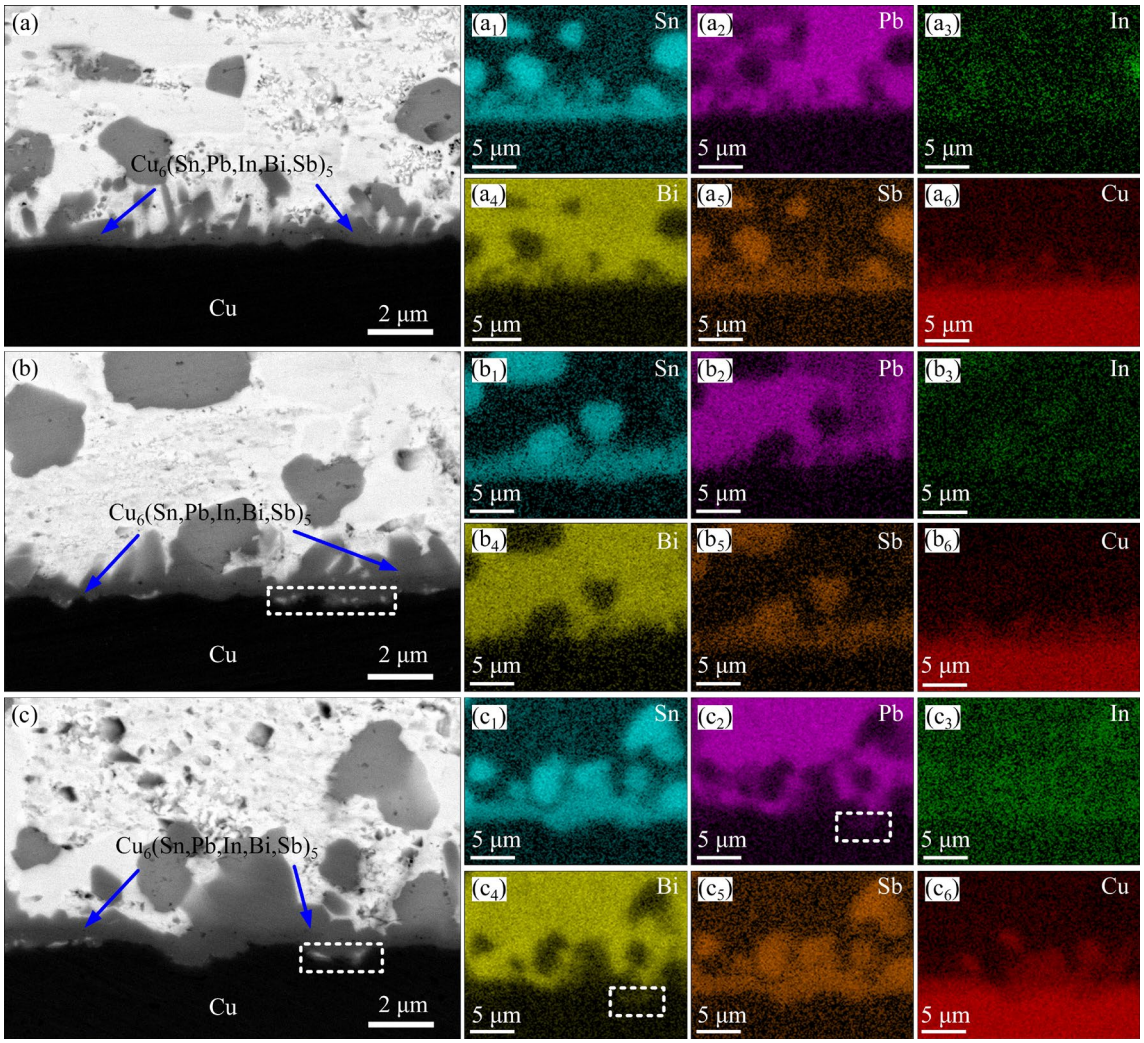

Fig. 5 Elemental distribution of Cu/SnPbInBiSb reaction interface after reflowing at different parameters: (a, a_1−a_6) 160 °C, 10 min; (b, b_1−b_6) 180°C, 10 min; (c, c_1−c_6) 200 °C, 10 min

elements, and also contained a small amount of Pb, Bi and In elements. With the increase of reflowing temperature, the Pb and Bi elements gradually diffused into the interface between IMC and Cu substrate as proved in Figs. 5(c, c_2, c_4). Due to the fact that Pb and Bi elements did not have metallurgical reaction with Cu, the dense distribution of Pb and Bi elements in the front of reaction interface actually worked as a diffusion barrier which restrained the diffusion of Cu atoms. To clearly describe the diffusion behavior of multiple elements, the diffusion process between solid Cu substrate and liquid solder alloy was shown in Fig. 6. This schematic diagram displayed the diffusion behavior of atoms dissolved at the solid−liquid interface of Cu/Sn-based solder alloy and Cu/SnPbInBiSb solder alloy. In the liquid solder, the medium-range order (MRO) structure of Cu_6Sn_5-type cluster existed and served as the potential nuclei for the formation of Cu_6Sn_5-type IMC [30]. The existence of Cu_6Sn_5-type MRO clusters could also accelerate the growth rate of IMC. In Fig. 6(a), the Sn atoms in the liquid Sn-based solder alloys usually occupied the dominant reaction with Cu atoms. Due to the higher concentration of the Cu and Sn elements, the formation rate and the amount of Cu_6Sn_5-type MRO clusters both increased. However, in Fig. 6(b), the components of atoms in liquid SnPbInBiSb solder were complex. In the front of the solid−liquid interface, a certain amount of Cu, Sn, Pb, In, Bi and Sb atoms were randomly diffused. According to the Richard's rule, when a solid metal melted into liquid state, the entropy will increase 1R (R means molar gas constant) [31]. This high entropy state of the liquid reaction layer might hinder the formation rate of Cu_6Sn_5-type MRO clusters and reduce the growth rate of IMCs [30], which means that the high entropy liquid SnPbInBiSb solder could still have the sluggish diffusion effect and impede the interdiffusion of Cu and Sn atoms. The other researcher also proved that the sluggish diffusion effect of liquid high entropy alloy still worked [5].

To reveal the constituent of the formed IMC, the chemical compositions of these IMCs listed in Table 1 were analyzed in Fig. 7. As shown in Fig. 7, the content of Cu element in most of the detected points was 50 at.%−60 at.%, and the content of Sn element was occupied 30 at.%−40 at.%, then the remaining content was taken up by Pb, In, Bi and Sb atoms. The total content of Pb, In, Bi and Sb in IMC steadily made up 5 at.%−15 at.%, as shown in Fig. 7(d). It can be empirically deduced that almost all the IMCs formed in the Cu/SnPbInBiSb/Cu solder joints belong to the basic type of Cu_6Sn_5, with a certain proportion of Pb, In, Bi and Sb elements dissolved in them. Considering the obvious decrease of Sn molar ratio in Cu_6Sn_5, there is a possibility that the atoms of Pb, In, Bi and Sb replace the Sn atoms in the lattice of Cu_6Sn_5, thus forming a new metastable type of IMC $Cu_6(Sn,Pb,In,Bi,Sb)_5$. Furthermore, the dissolution of a certain amount of Pb, In, Bi and Sb atoms into the lattice structure of Cu_6Sn_5 would possibly distort the original lattice structure. The distorted structure of $Cu_6(Sn,Pb,In,Bi,Sb)_5$ could hinder the interdiffusion between reaction atoms, thus restraining the growth of IMC.

As shown in Fig. 8 and Fig. 9, the interface of Cu/SnPbInBiSb solder joint reflowed at 180 °C for 10 min was observed by TEM to precisely analyze the structure and confirm the real types of

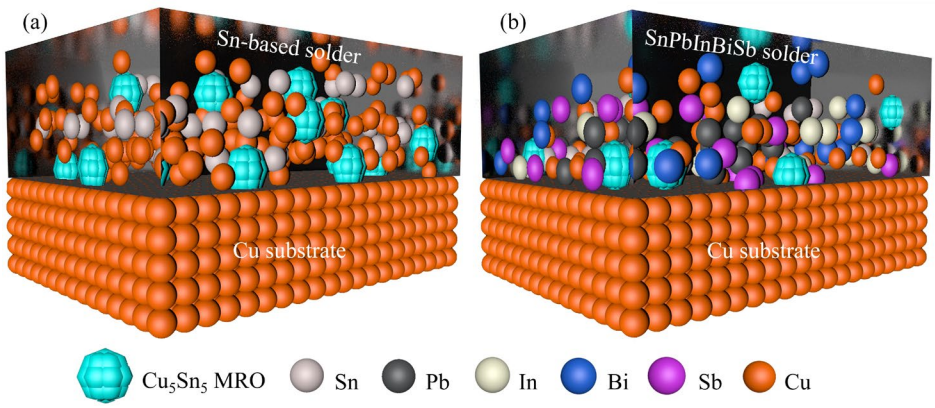

Fig. 6 Diffusion mechanism of Cu/solder alloy solid−liquid interface: (a) Cu/Sn based solder; (b) Cu/SnPbInBiSb solder

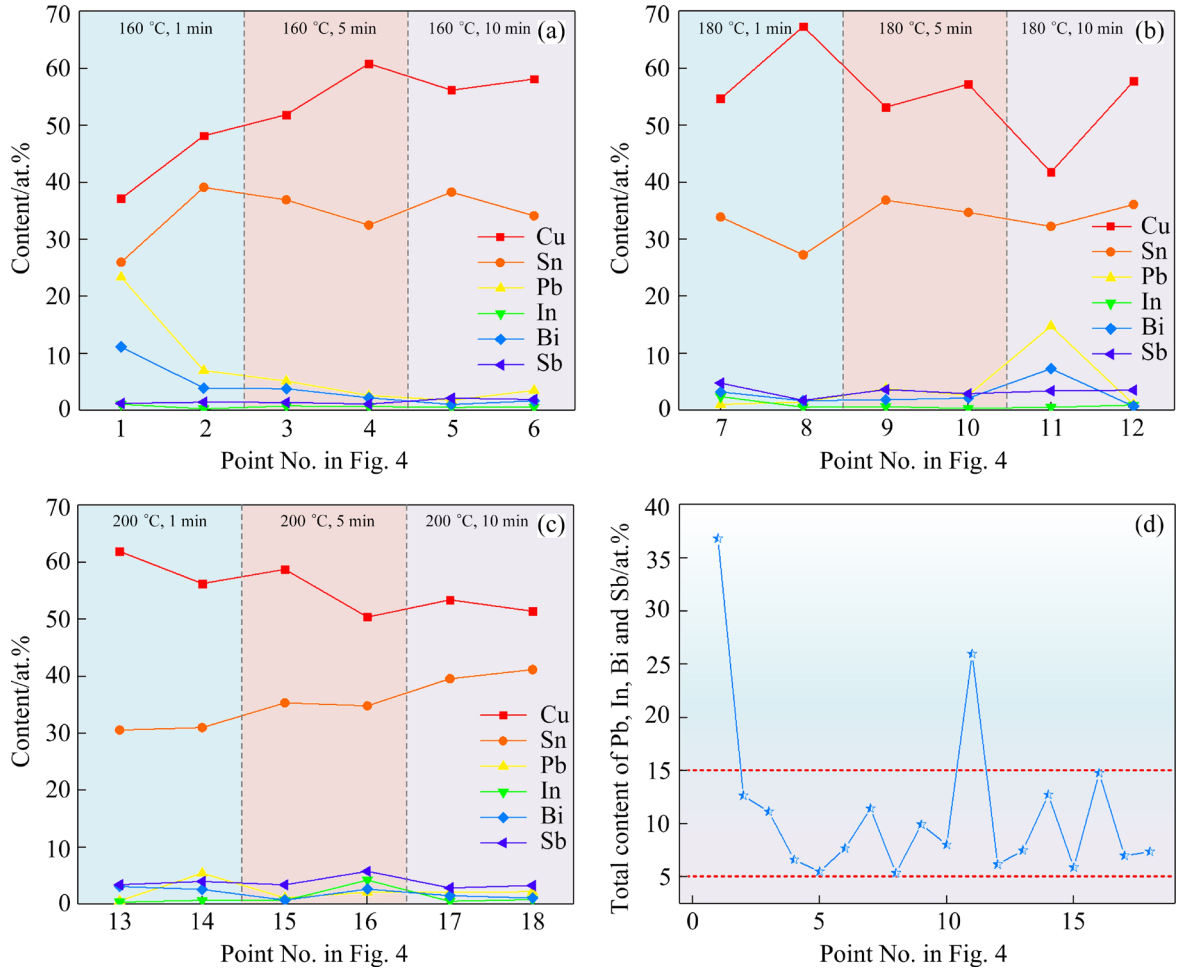

Fig. 7 Chemical compositions of IMC marked in solder joints reflowed at different temperatures of 160 °C (a), 180 °C (b) and 200 °C (c), and total content of Pb, In, Bi and Sb (d)

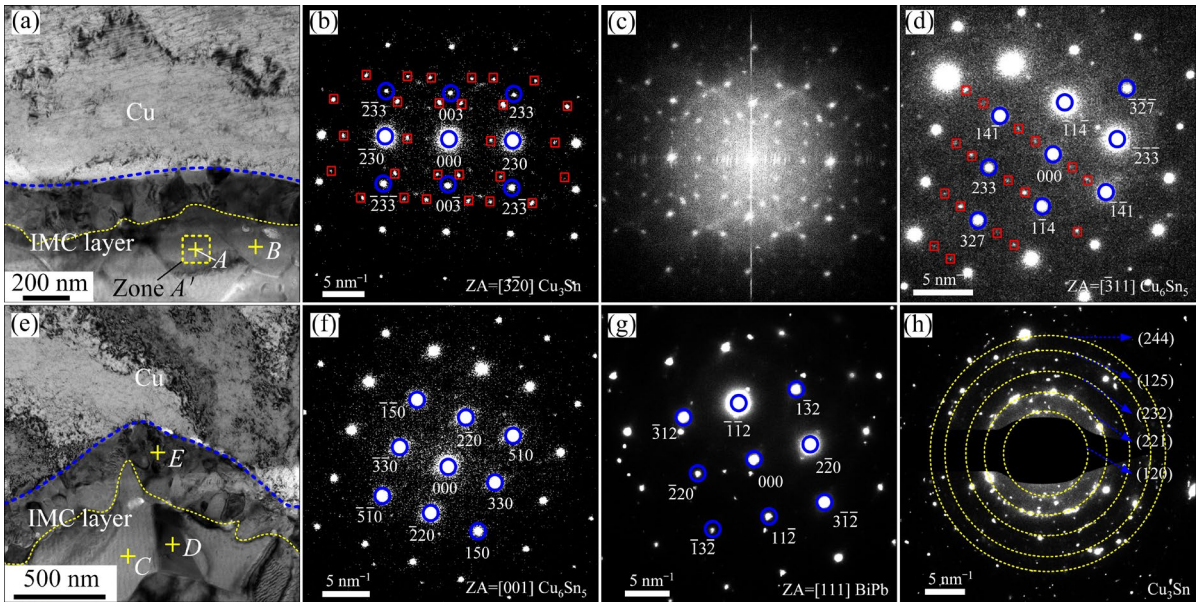

Fig. 8 TEM images of solder joint reflowed at 180 °C for 10 min: (a) Bright field image of Cu/IMC interface; (b) SAED pattern of Point *A*; (c) FFT pattern of Zone *A′*; (d) SAED pattern of Point *B*; (e) Another bright field image of Cu/IMC interface; (f) SAED pattern of Point *C*; (g) SAED pattern of Point *D*; (h) SAED pattern of Point *E*

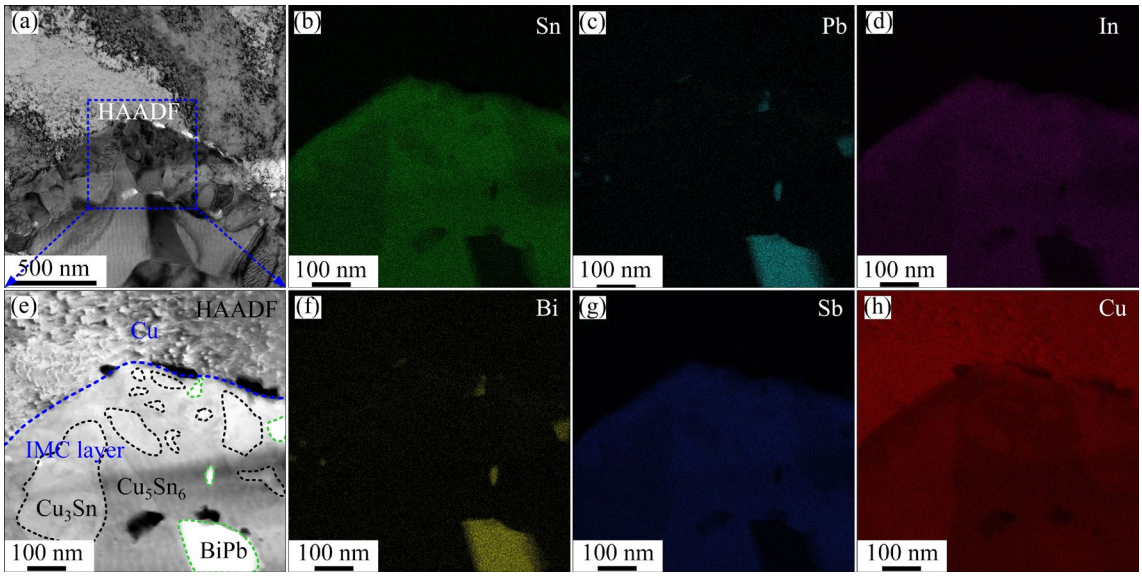

Fig. 9 Elemental distribution of Cu/IMC interface: (a) Bright field image; (b) Distribution of Sn element; (c) Distribution of Pb element; (d) Distribution of In element; (e) Dark field image of marked area in (a); (f) Distribution of Bi element; (g) Distribution of Sb element; (h) Distribution of Cu element

IMCs. The SAED patterns of the interfacial IMCs was detected and indexed as presented in Fig. 8. In the bright field images of Figs. 8(a) and (e), it could be seen that the aforementioned metastable IMC $Cu_6(Sn,Pb,In,Bi,Sb)_5$ layer was actually composed of two layers. The first layer of IMC was adjacent to Cu substrate with smaller grains of Cu_3Sn (Point *E*), and the second layer of IMC was composed of larger grains of Cu_6Sn_5 (Points *B* and *C*), Cu_3Sn (Point *A*) and BiPb (Point *B*). Moreover, the SAED patterns of Points *A* and *B* showed the extra ordered structure marked by red boxes. In Fig. 8(c), the fast Fourier transform (FFT) of the high-resolution TEM of Point *A* also confirmed that the ordered structure of Point *A* authentically existed and was not caused by the overlap of multiphase. These ordered superlattice structures of Cu_3Sn and Cu_6Sn_5 may be caused by the dissolution of other atoms.

The high-angle annular dark field (HAADF) image was captured and the elemental distribution was detected as shown in Fig. 9. From the image of HAADF in Fig. 9(e), it can be seen that the first IMC layer contained Cu_6Sn_5, Cu_3Sn and BiPb phases. The Cu_3Sn and BiPb phases were randomly distributed on the matrix of Cu_6Sn_5. Moreover, the compositions of the Cu_6Sn_5 and Cu_3Sn phases contained In and Sb elements. And the distribution density of In and Sb elements in Cu_6Sn_5 phase was higher than that in Cu_3Sn phase. The dissolved In and Sb elements actually might replace the Sn atoms in the lattice structures of Cu_6Sn_5 and Cu_3Sn. Due to the difference of the atomic radius among Sn and In, and Sb atoms, the original lattice structures of Cu_6Sn_5 and Cu_3Sn phases could be distorted. This lattice-distorted IMC layer could further hinder the diffusion of Cu atoms. After investigating the diffusion process of reaction atoms and the growth behavior of IMCs, it can be concluded that the low growth rate of IMCs formed at the Cu/SnPbInBiSb interface was not only related to the high entropy state of the liquid SnPbInBiSb solder, but also concerned with the complex structure of IMCs.

3.3 Growth kinetics of complex intermetallic compound

To further reveal the growth kinetics of the IMCs, the average thickness of the whole IMC layer was measured and analyzed. The thickness data of IMC in our previous work [24] and this work was both counted and calculated. The equation of IMC growth is listed below [20]:

$$L=Dt^n \tag{1}$$

This empirical equation shows the relationship between average thickness (L), reaction time (t) and growth rate (D). The exponent (n) is a reaction constant which is highly related to the growth mechanism of IMC. Moreover, the relationship between growth rate D and thermodynamic

temperature (T) can be described by the following Arrhenius equation [20]:

$$D = A\exp\left(-\frac{E_a}{RT}\right) \quad (2)$$

where A is a constant, R is the molar gas constant, and E_a is the activation energy. The average thickness L and reaction time t were fitted into the logarithm of Eq. (1) to calculate the exponent n. As shown in Fig. 10(a), the fitting results of exponent n at reaction temperatures of 160, 180 and 200 °C were 0.27±0.07, 0.42±0.01 and 0.40, respectively. Then, the experimental value of exponent n was close to be 1/3, thus indicating that the metastable IMC formed in the interfacial reaction between Cu and liquid SnPbInBiSb was controlled by ripening growth kinetics [32]. In Fig. 10(b), the growth rate D at different reflowing temperatures was calculated by fitting Eq. (1) with the average thickness data of IMC and $t^{1/3}$. The value of growth rate D increased with the rise of reflowing temperature. Moreover, the fitting result of activation energy E_a is 40.9 kJ/mol, as shown in Figs. 10(c, d). Compared with published data of E_a for Cu−Sn [33], Cu−Sn58Bi [20], Cu−Sn37Pb [34], and Cu−SnBiInZn [5] solid−liquid interfacial reaction, the activation energy of Cu/SnPbInBiSb is much higher than these published data. Generally, the higher the activation energy is, the slower the formation rate of IMC is. This high activation energy of Cu/SnPbInBiSb solid−liquid reaction couple is also responsible for the very low growth behavior of the whole IMC layer. All in all, compared with the solid−liquid interfacial reaction of the Cu−Sn-based solder alloy, the solid−liquid interfacial reaction between Cu substrate and SnPbInBiSb high entropy solder alloy was obviously suppressed. Moreover, this ability of restraining the overgrowth of IMCs indicates that SnPbInBiSb solder alloy has potential to be applied in the advanced electronic packaging.

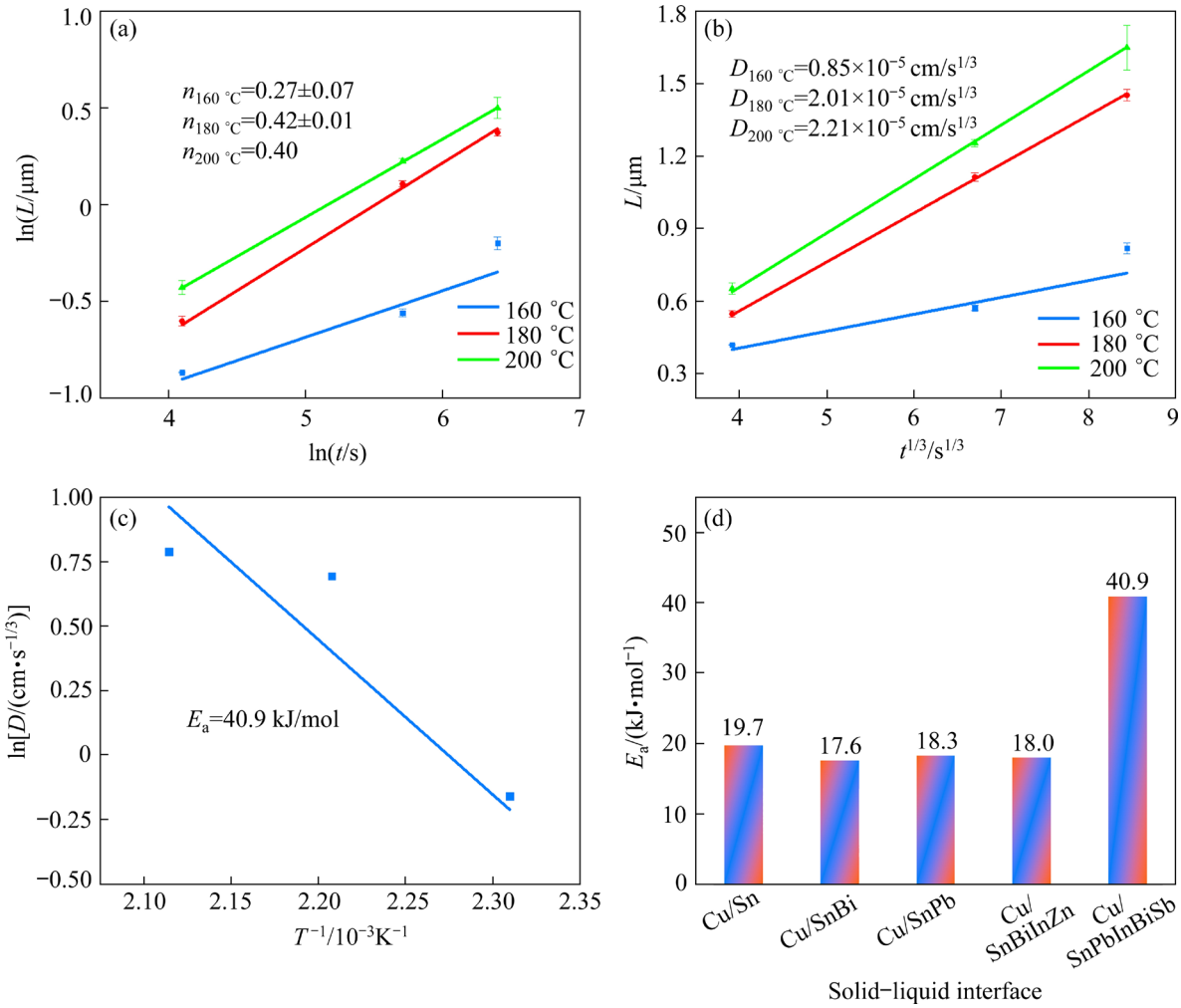

Fig. 10 Growth kinetic plots of IMC formed at Cu/SnPbInBiSb interface: (a) ln L−ln t; (b) L−$t^{1/3}$; (c) ln D−T^{-1}; (d) Comparison of activation energy in different solder joints

4 Conclusions

(1) A new type of high entropy solder alloy SnPbInBiSb was fabricated and the interfacial reaction of Cu/SnPbInBiSb/Cu sandwich joints was investigated.

(2) After the reflowing process, a layer of complex IMC $Cu_6(Sn,Pb,In,Bi,Sb)_5$ formed at the Cu/SnPbInBiSb interface. The grains of this IMC kept in columnar shape rather than lamellar shape and the maximum average thickness of the IMC layer was only 1.66 μm in the solder joints reflowed at 200 °C for 10 min.

(3) During the reflow process, the high entropy state of the liquid reaction layer might hinder the formation rate of Cu_6Sn_5-type medium range order clusters and reduce the growth rate of the complex IMC.

(4) This complex IMC layer was actually composed of BiPb, Cu_6Sn_5 and Cu_3Sn phases. The In and Sb elements dissolved in the structure of Cu_6Sn_5 and Cu_3Sn phases, thus distorting the original lattice structure and impeding the diffusion of Cu atoms from Cu substrate into liquid solder.

(5) The activation energy of Cu/SnPbInBiSb solid−liquid interfacial reaction reached up to 40.9 kJ/mol, much higher than that of other Sn-based solder. The high activation energy is the primary cause of the sluggish diffusion of reaction atoms and slow growth of the IMC formed in Cu/SnPbInBiSb/Cu sandwich joints.

CRediT authorship contribution statement

Shuai WANG: Conceptualization, Methodology, Investigation, Writing − Original draft; **Jia-yun FENG:** Writing − Review & editing, Supervision; **Wei WANG:** Investigation, Data curation; **Wen-chao CAO** and **Xin DING:** Methodology, Investigation; **Shang WANG:** Investigation, Resources, Supervision; **Yan-hong TIAN:** Resources, Supervision, Project administration, Funding acquisition.

Declaration of competing interest

The authors declare that they have no known competing financial interests or personal relationships that could have appeared to influence the work reported in this paper.

Acknowledgments

This work was supported by the National Natural Science Foundation of China (No. U2241223), the Heilongjiang Touyan Innovation Team Program, China (No. HITTY-20190013), and the Fundamental Research Funds for the Central Universities, China (No. AUEA5770400622).

References

[1] LAU J H. State-of-the-art and outlooks of chiplets heterogeneous integration and hybrid bonding [J]. Journal of Microelectronics and Electronic Packaging, 2021, 18(4): 145−160.

[2] LAU J H. Recent advances and trends in heterogeneous integrations [J]. Journal of Microelectronics and Electronic Packaging, 2019, 16(2): 45−77.

[3] TU K N. Reliability challenges in 3D IC packaging technology [J]. Microelectronics Reliability, 2011, 51(3): 517−523.

[4] LIU Y, TU K N. Low melting point solders based on Sn, Bi, and In elements [J]. Materials Today Advances, 2020, 8: 100115.

[5] LIU Y, PU L, YANG Y, HE Q, ZHOU Z, TAN C, ZHAO X, ZHANG Q, TU K N. A high-entropy alloy as very low melting point solder for advanced electronic packaging [J]. Materials Today Advances, 2020, 7: 100101.

[6] HARIHARAN G, CHAWARE R, SINGH I, LIN J, YIP L, NG K, PAI S Y. A comprehensive reliability study on a CoWoS 3D IC package [C]//Proceedings of the IEEE 65th Electronic Components and Technology Conference (ECTC). San Diego: IEEE, 2015: 573−577.

[7] NIU Yu-ling, WANG Hua-yan, SHAO Shuai, PARK S B. In-situ warpage characterization of BGA packages with solder balls attached during reflow with 3D digital image correlation (DIC) [C]//Proceedings of the IEEE 66th Electronic Components and Technology Conference (ECTC). Las Vegas: IEEE, 2016: 782−788.

[8] HUA F, MEI Z Q, GLAZER J. Eutectic Sn-Bi as an alternative to Pb-free solders [C]//Proceedings of the 48th Electronic Components and Technology Conference. Seattle: IEEE, 1998: 277−283.

[9] SHEN Lu, FOO A Q, WANG Shi-jie, CHEN Zhong. Enhancing creep resistance of SnBi solder alloy with non-reactive nano fillers: A study using nanoindentation [J]. Journal of Alloys and Compounds, 2017, 729: 498−506.

[10] CHANTARAMANEE S, SUNGKHAPHAITOON P. Combined effects of Bi and Sb elements on microstructure, thermal and mechanical properties of Sn−0.7Ag−0.5Cu solder alloys [J]. Transactions of Nonferrous Metals Society of China, 2022, 32(10): 3301−3311.

[11] LIU P L, SHANG J K. Interfacial segregation of bismuth in copper/tin-bismuth solder interconnect [J]. Scripta Materialia, 2001, 44(7): 1019−1023.

[12] ZHU Wen-bo, MA Yong, LI Xue-zheng, ZHOU Wei, WU Ping. Effects of Al_2O_3 nanoparticles on the microstructure and properties of $Sn_{58}Bi$ solder alloys [J]. Journal of Materials Science: Materials in Electronics, 2018, 29: 7575−7585.

[13] GAIN A K, ZHANG L C. Interfacial microstructure, wettability and material properties of nickel (Ni) nanoparticle doped tin−bismuth−silver (Sn−Bi−Ag) solder on copper (Cu) substrate [J]. Journal of Materials Science: Materials in Electronics, 2016, 27: 3982−3994.

[14] LI Xue-zheng, MA Yong, ZHOU Wei, WU Ping. Effects of nanoscale Cu_6Sn_5 particles addition on microstructure and properties of SnBi solder alloys [J]. Materials Science and

Engineering A, 2017, 684: 328−334.
[15] YANG Li, ZHU Lu, ZHANG Yao-cheng, ZHOU Shi-yuan, WANG Guo-qiang, SHEN Sai, SHI Xiao-long. Microstructure, IMCs layer and reliability of Sn−58Bi solder joint reinforced by Mo nanoparticles during thermal cycling [J]. Materials Characterization, 2019, 148: 280−291.
[16] MIAO Hui-wei, DUH J G, CHIOU B S. Thermal cycling test in Sn−Bi and Sn−Bi−Cu solder joints [J]. Journal of Materials Science: Materials in Electronics, 2000, 11: 609−618.
[17] XU Heng, LUO Deng-jun, YAN Yan-hong, LI Shou-wei, GAO Na-yan. Effects of addition of trace elements on the structure and properties of multicomponent Sn−Bi based solder alloys [J]. Micronanoelectronic Technology, 2021, 58(2): 124−130.
[18] SONG Qian-qian, LI An-min, QI Da, QIN Wei-ou, LI Yi-tai, ZHAN Yong-zhong. Interface reaction and mechanical properties of $Sn_{58}Bi$−XCr/$Cu_{30}Zn(Cu_7Sn)$solder joints under isothermal aging conditions[J]. Intermetallics, 2022, 150: 107696.
[19] MA Yong, LI Xue-zheng, YANG Li-zhuang, ZHOU Wei, WANG Ming-xia, ZHU Wen-bo, WU Ping. Effects of graphene nanosheets addition on microstructure and mechanical properties of SnBi solder alloys during solid-state aging [J]. Materials Science and Engineering A, 2017, 696: 437−444.
[20] LI J F, MANNAN S H, CLODE M P, WHALLEY D C, HUTT D A. Interfacial reactions between molten Sn−Bi−X solders and Cu substrates for liquid solder interconnects [J]. Acta Materialia, 2006, 54(11): 2907−2922.
[21] ZHANG Yong, ZUO T T, TANG Z, GAO M C, DAHMEN K A, LIAW P K, LU Z P. Microstructures and properties of high-entropy alloys [J]. Progress in Materials Science, 2014, 61: 1−93.
[22] YEH J W. Recent progress in high entropy alloys [J]. Ann Chim Sci Mat, 2006, 31(6): 633−648.
[23] WANG Shuai, FENG Jia-yun, WANG Shang, WANG Kai-feng, YU Mu-ying, TIAN Yan-hong. Interfacial reaction between novel high entropy alloy SnPbInBiSb and Cu substrate [J]. Materials Letters, 2022, 325: 132901.
[24] WANG Shuai, FENG Jia-yun, SA Zi-cheng, WANG Yi-ping, WANG Shang, TIAN Yan-hong. Interfacial reaction of Cu/SnPbInBiSb/Cu sandwich solder joints [C]//Proceedings of the 23rd International Conference on Electronic Packaging Technology (ICEPT). Dalian: IEEE, 2022: 1−5.
[25] SHANG P J, LIU Z Q, LI D X, SHANG J K. Bi-induced voids at the Cu_3Sn/Cu interface in eutectic SnBi/Cu solder joints [J]. Scripta Materialia, 2008, 58(5): 409−412.
[26] BASHIR M N, HASEEB A S M A. Grain size stability of interfacial intermetallic compound in Ni and Co nanoparticle-doped SAC305 solder joints under electromigration [J]. Journal of Materials Science: Materials in Electronics, 2022, 33(17): 14240−14248.
[27] LIU Zhi-yuan, MA Hao-ran, SHANG Sheng-yan, WANG Yun-peng, LI Xiao-gan, MA Hai-tao. Effects of TiO_2 nanoparticles addition on physical and soldering properties of Sn−$x$$TiO_2$ composite solder [J]. Journal of Materials Science: Materials in Electronics, 2019, 30: 18828−18837.
[28] HU Xiao-wu, QIU Hong-yu, JIANG Xiong-xin. Effect of Ni addition into the Cu substrate on the interfacial IMC growth during the liquid-state reaction with Sn−58Bi solder [J]. Journal of Materials Science: Materials in Electronics, 2019, 30: 1907−1918.
[29] SON J, KIM M, YU D Y, KO Y H, YOON J W, LEE C W, PARK Y B, BANG J. Thermal aging characteristics of Sn−xSb solder for automotive power module [J]. Journal of Welding and Joining, 2017, 35(5): 38−47.
[30] ZHAO Ning, PAN Xue-min. Liquid structure of Sn−Ag−xCu solders and its effect on the formation and growth of interfacial Cu_6Sn_5 [J]. Journal of Materials Science, 2020, 55: 13294−13302.
[31] GAO M C, YEH J W, LIAW P K, ZHANG Y. High-entropy alloys [M]. Cham: Springer International Publishing, 2016.
[32] SALLEH M M A A, MCDONALD S D, YASUDA H, SUGIYAMA A, NOGITA K. Rapid Cu_6Sn_5 growth at liquid Sn/solid Cu interfaces [J]. Scripta Materialia, 2015, 100: 17−20.
[33] LI J F, AGYAKWA P A, JOHNSON C M. Interfacial reaction in Cu/Sn/Cu system during the transient liquid phase soldering process [J]. Acta Materialia, 2011, 59(3): 1198−1211.
[34] SLATER J C. Atomic radii in crystals [J]. The Journal of Chemical Physics, 1964, 41(10): 3199−3204.

铜基体上 SnPbInBiSb 高熵钎料焊点界面金属间化合物的生长动力学

王 帅[1]，冯佳运[1]，王 玮[1]，曹文超[2]，丁 鑫[2]，王 尚[1]，田艳红[1,3]

1. 哈尔滨工业大学 材料结构精密焊接与连接全国重点实验室，哈尔滨 150001；
2. 哈尔滨工业大学 金属精密热加工国家级重点实验室，哈尔滨 150001；
3. 哈尔滨工业大学 郑州研究院，郑州 450041

摘 要：研究低温长时间回流后高熵钎料 Cu/SnPbInBiSb 焊点界面复杂金属间化合物(IMCs)的生长行为，并揭示 Cu/SnPbInBiSb 固−液反应界面 IMCs 生长的抑制机理。研究发现，在 Cu/SnPbInBiSb 固−液反应界面形成的复杂 IMC 生长速度明显减慢。在最高回流温度 200 ℃回流 10 min 后界面 IMCs 的最大平均厚度仅为 1.66 μm。复杂 IMCs 缓慢生长的机理归纳为三点：首先，液态 SnPbInBiSb 高熵钎料的高熵状态降低了复杂 IMCs 的生长速率；其次，复杂 IMC 变形的晶格结构阻碍了 Cu 原子的扩散；最后，Cu/SnPbInBiSb 固−液界面反应具有更高的激活能(40.9 kJ/mol)，实质上阻碍了复杂 IMCs 的生长。

关键词：高熵合金；界面反应；显微组织演变；生长动力学；金属间化合物

(Edited by Wei-ping CHEN)